JOC The Journal of Organic Chemistry

Article

Synthesis of a family of highly substituted porphyrin thioethers via nitro displacement in 2,3,7,8,12,13,17,18-octaethyl-5,10,15,20-tetranitroporphyrin

Marc Kielmann, Keith J. Flanagan, Karolis Norvaiša, Daniela Intrieri, and Mathias O. Senge

J. Org. Chem., **Just Accepted Manuscript** • Publication Date (Web): 28 Apr 2017

Synthesis of a family of highly substituted porphyrin thioethers *via* nitro displacement in 2,3,7,8,12,13,17,18-octaethyl-5,10,15,20-tetranitroporphyrin.

Marc Kielmann, Keith J. Flanagan, Karolis Norvaiša, Daniela Intrieri and Mathias O. Senge*

School of Chemistry, SFI Tetrapyrrole Laboratory, Trinity Biomedical Sciences Institute, Trinity College Dublin, the University of Dublin, 152-160 Pearse St., Dublin 2, Ireland.

ABSTRACT: A series of highly substituted porphyrin thioethers was synthesized from 2,3,7,8,12,13,17,18-octaethyl-5,10,15,20-tetranitroporphyrin (H_2OETNP). The reactions proceeded *via* a S_NAr mechanism with a broad range of aromatic thiols in the presence of a base. This is a rapid way to prepare a large variety of meso-substituted porphyrins from only one precursor. Single crystal X-ray analysis revealed that these new porphyrin thioethers are highly distorted, exhibiting conformational properties which are distinctive of both meso-sulfur substitution and steric overcrowding in general. Additionally, denitration of H_2OETNP under basic conditions was investigated, yielding products of stepwise desubstitution. This allowed a comparative X-ray crystallographic study to delineate the successive structural effects of an increasing degree of nitro substitution in the complete series of nitro-substituted octaethylporphyrins.

INTRODUCTION

Modification of the porphyrin macrocycle *via* substitution reactions, for example with organolithium reagents,[1] allows tailoring the tetrapyrrole scaffold for a plethora of applications. Likewise, variation of the peripheral substitution pattern of highly substituted porphyrins, such as 2,3,7,8,12,13,17,18-octaethyl-5,10,15,20-tetranitroporphyrin H_2OETNP (**1**),[2] may be utilized to access new derivatives with interesting and unique chemical and photophysical properties and the H_2OETNP framework has found frequent use in studies on nonplanar porphyrins, π-aggregation, and supramolecular chemistry.[3] Nitroporphyrins have been reported to undergo nucleophilic aromatic substitution (S_NAr) in the presence of halides,[2] amines,[4] and

azide.[4] This is due to the presence of the highly electron-withdrawing nitro substituents and the ability of nitro groups to serve as leaving groups. The substitution proceeds *via* an addition-elimination mechanism, in which a delocalized and stabilized anion is generated and elimination of the leaving group results in formation of the substituted product.[3]

Substitutions involving sulfur nucleophiles usually require a number of prerequisites, such as activating groups, high temperatures or metal catalysts.[5] As a result, catalyst-free S_NAr reactions at the meso-positions of tetrapyrroles are scarce,[1,6] but it was briefly reported that thiolate anions substitute nitro groups on porphyrins.[7] Recently, we reported on sulfur-linked porphyrin dimers involving S_NAr reactions of porphyrin thiolates under mild conditions, where seemingly unactivated systems gave excellent yields.[6b]

This inspired us to synthesize a family of porphyrin thioethers carrying a high number of meso-arylthio substituents as a new class of highly substituted porphyrins.[8] Such compounds might be suitable for biological and medicinal applications due to the presence of sulfur[9] or applicable as porphyrin-based self-assembled monolayers (SAMs) on gold surfaces.[10] Interest in such systems is now expanding to other porphyrinoids as well.[11] Herein, we describe the ability of a broad range of aromatic thiolates to participate in substitution reactions under mild conditions, conveniently without protective atmosphere. Furthermore, thiolates can participate in reductions of nitroporphyrins, competing with the substitution process. Hence, H_2OETNP (**1**) was presumed to represent a good starting point for further investigations on this ambivalent thiolate reactivity: As will be shown, while porphyrin **1** was rapidly (often <5 min) tetrasubstituted by many nucleophilic thiolates, denitration occurred preferably with the sulfur reagents **HSAr[12]**–**HSAr[14]** (Scheme 1). This is intriguing, as comparable desubstitutions of meso-positions are limited to only few examples.[7a,12]

Scheme 1. Reaction of nitroporphyrins with thiolates: Substitution *versus* reduction.

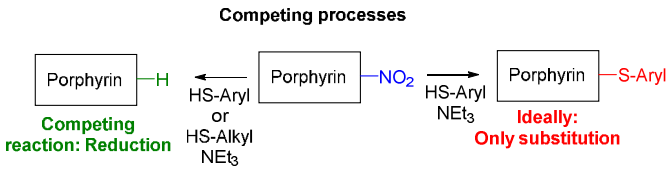

RESULTS AND DISCUSSION

Synthetic Studies

Highly Substituted Porphyrin Thioethers. To establish a standard protocol for the synthesis of highly substituted arylthioporphyrins derived from the parent compound H_2OETNP (**1**) and to generate a library of such molecules, the reactivity of a large number of aromatic thiolates was investigated. Initial screening experiments were performed with 4-bromobenzenethiol. Thus, when compound **1** was reacted with an excess of HSAr[1] in boiling chloroform in the absence of a base, the products **2**–**5** were formed (Scheme 2). Presumably, the thiolate needed for reaction originated from a thiol-thiolate equilibrium in solution.

Scheme 2. Reaction of H_2OETNP (1) with 4-bromobenzenethiol (HSAr[1]) in the absence of a base.

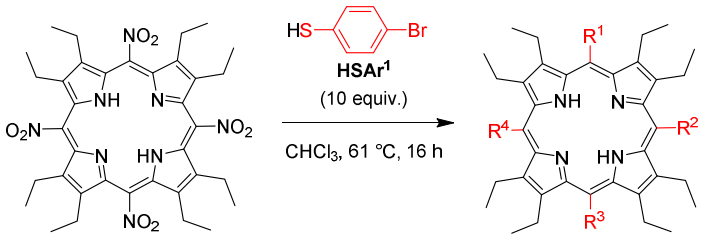

2 $R^1 = R^2 = R^3 = R^4 = SAr^1$ (52%)
3 $R^1 = R^2 = R^3 = SAr^1$, $R^4 = H$ (30%)
4 $R^1 = R^2 = SAr^1$, $R^3 = R^4 = H$ (10%)[a]
5 $R^1 = R^3 = SAr^1$, $R^2 = R^4 = H$ (6%)[a]

[a] An inseparable 3:2 mixture of compounds **4** and **5** was isolated.

Screening of a range of thiolate nucleophiles was conducted and the use of TEA allowed for shorter reaction times and lower temperatures with most reactions being complete within minutes. Furthermore, the number of equivalents of thiol used could be

reduced in many cases. A good example is the synthesis of porphyrin **2**: While the dodecasubstituted product was formed in 52% yield along with 30% of the undecasubstituted porphyrin **3** in the absence of base under harsh conditions (Scheme 2), the same product was obtained in 73% yield under basic conditions along with less than 10% of **3** (Scheme 3).

A series of experiments, in which H_2OETNP (**1**) and **HSAr**[1] were reacted in the presence of varying amounts of TEA, revealed that rapid (<5 min) and complete conversion of **1** was achieved once a threshold of 50 mol-% TEA (relating to the thiol) was maintained. Hence, three drops of TEA (corresponding to ~0.27 mmol) were used in each substitution reaction from that point for synthetic ease (for full detail see SI: Table S1).

Scheme 3. S_NAr on H_2OETNP (1) using various sulfur nucleophiles (HSAr[1]–HSAr[11]).

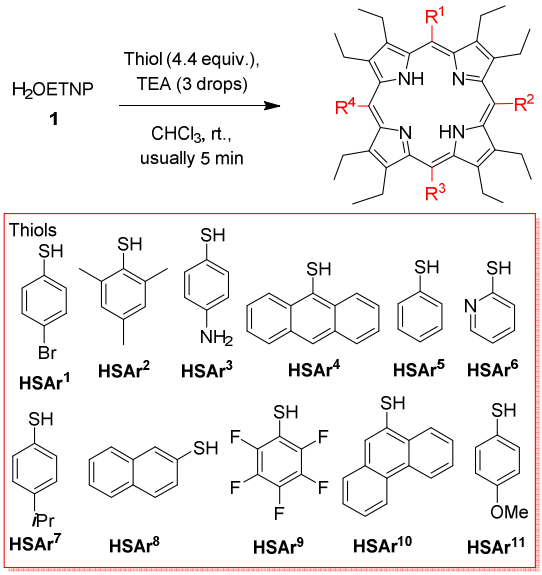

Entry	R^1	R^2	R^3	R^4	Product	Yield, %
1	SAr^1	SAr^1	SAr^1	SAr^1	**2**	73
2	SAr^2	SAr^2	SAr^2	H	**6**	40
3[a]	SAr^3	SAr^3	SAr^3	H	**7**	40
4[b]	SAr^4	SAr^4	SAr^4	H	**8**	35
5	SAr^5	SAr^5	SAr^5	SAr^5	**9**	86
6	SAr^6	SAr^6	SAr^6	SAr^6	**10**	65
7	SAr^7	SAr^7	SAr^7	SAr^7	**11**	63

8	SAr^{8}	SAr^{8}	SAr^{8}	SAr^{8}	**12**	46
9	SAr^{9}	SAr^{9}	SAr^{9}	SAr^{9}	**13**	43
10	SAr^{10}	SAr^{10}	SAr^{10}	SAr^{10}	**14**	17
11	SAr^{11}	SAr^{11}	SAr^{11}	H	**15**	<5[c]
12	SAr^{11}	SAr^{11}	SAr^{11}	SAr^{11}	**16**	<5[c]

[a] 7.8 equiv. of **HSAr[3]** were used. [b] 8.8 equiv. of **HSAr[4]** were used. [c] Obtained as a mixture of **15** and **16** and identified by HRMS only due to the small amount of material obtained.

Conversion of **1** with a number of electron-deficient and electron-rich aromatic thiols (**HSAr[2]**–**HSAr[11]**) resulted in the formation of highly substituted products (**6**–**16**) with yields of up to 86% for the phenylthio-substituted species **9** (Scheme 3) and we propose an addition-elimination mechanism in which a Jackson-Meisenheimer complex[1,2,13] is formed. In order to optimize the outcome of each reaction, the number of equivalents of thiol used and reaction time had to be increased in some cases. Formation of compounds **3**–**8** and **15** reveals the ambivalence of some thiolates to both substitute and reduce the meso-positions in the nitroporphyrin **1**. Differences in the reactivity and probably steric demand of the sulfur reagents determined that in some cases only the trisubstituted product was isolated.

To study the effects of the central metal, the nickel complex **17** was reacted with **HSAr[6]** in a test reaction. As a result, **18** and **19** were obtained as products from the same reaction, along with unreacted starting material. Interestingly, substitution was less prominent compared to the free base and denitration prevailed. Electrochemical data suggest that Ni(II)porphyrins are generally more difficult to reduce[14] and better electrophiles.[4] Remarkably, the unsymmetric undecasubstituted tetrapyrrole **19** was formed in only one step from **17** *via* desymmetrization (Scheme 4).

Scheme 4. Reaction of Ni(II)porphyrin 17 and 2-mercaptopyridine (HSAr[6]).

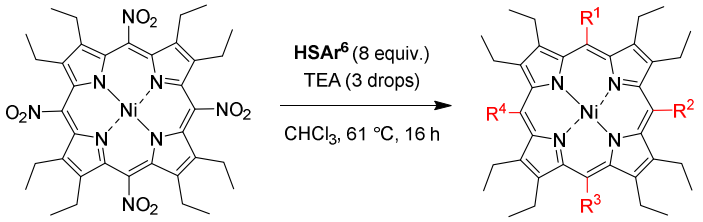

18 $R^1 = R^2 = NO_2$, $R^3 = R^4 = H$ (25%)
19 $R^1 = R^2 = NO_2$, $R^3 = SAr^6$, $R^4 = H$ (20%)

Stepwise Denitration of H_2OETNP. The frequent formation of desubstituted meso-positions in a number of reactions under involvement of the organosulfur reagents was investigated further during attempts to substitute **1** with the thiols **HSAr[12]**–**HSAr[14]**. Rather than substitution, a tendency towards desubstitution was observed and conditions for stepwise reduction were elaborated and optimized. In order to access the individual denitration products in good yield, it was necessary to increase the number of equivalents of thiol used and, in the case of **HSAr[13]** and **HSAr[14]**, the temperature. Treatment of **1** with 1,2-ethanedithiol (**HSAR[12]**) at r.t. gave dinitroporphyrins **20** and **21** and longer reaction times led to increased formation of **22** and eventually traces of **23**, while the reaction using 2-mercaptoethanol (**HSAr[13]**) in boiling DCM resulted in the formation of mononitroporphyrin **22** as main product with traces of **23** being formed at longer reaction times. Ultimately, **1** was reduced to 2,3,7,8,12,13,17,18-octaethylporphyrin (H_2OEP, **23**) in the presence of **HSAr[14]** (Scheme 5). Since formation of **23** occurred slowly as opposed to **20**–**22**, the reaction time had to be increased significantly. Despite all effort, such as decreasing the number of equivalents of thiolate used to one or less, no trinitro-substituted product was observed, presumably due to immediate additional denitration steps, once the species is formed. Instead of **32**, mostly unreacted starting material along with small amount of **20** and **21** was observed typically and further comparative studies on thiol reactivity were disregarded.

Scheme 5. Denitration of H_2OETNP (1) with thiols HSAr[12]–HSAr[14].

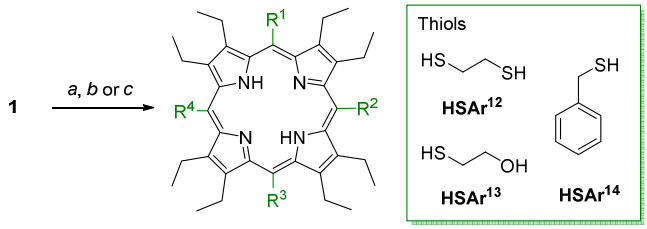

Entry	R^1	R^2	R^3	R^4	Product	Yield, %
1[a]	NO_2	H	H	NO_2	**20**	24
2[a]	NO_2	H	NO_2	H	**21**	21
3[b]	NO_2	H	H	H	**22**	49
4[c]	H	H	H	H	**23**	49

Reagents and conditions: [a] **HSAr[12]** (7 equiv.), TEA (3 drops), chloroform, r.t., 40 min. [b] **HSAr[13]** (12 equiv.), TEA (3 drops), DCM, 40 °C, 15 min. [c] **HSAr[14]** (41 equiv.), TEA (0.1 mL), DCM, 40 °C, 72 h.

These reactions proceeded rapidly, presumably due to the lower oxidation potential of alkyl thiols compared to aromatic thiols, which facilitated reduction of **1** to an extent that no substitution products could be isolated, even though alkyl thiolates are more nucleophilic. Note, that **20**–**22** are potential precursors for the preparation of nonplanar porphyrins with mixed substituents, which are of relevance for fundamental studies on the conformational flexibility of porphyrins.[8] It was also considered that in these cases, the basicity of TEA was insufficient to effectively deprotonate the sulfur reagents and initial studies on the reaction of **1** with **HSAr[12]**–**HSAr[14]** utilizing DBU and KO*t*Bu were conducted. However, these attempts were discontinued due to the formation of complex mixtures of inseparable products, potentially resulting from breakdown of the macrocycle.

A comparison of the substitution and denitration reactions indicates that both pathways are two independent reactions that contribute to the overall outcome of a conversion of **1** and a thiolate. The tendency to undergo either substitution or reductive desubstitution strongly depends on the reactivity of the sulfur reagents and how fast S_NAr proceeds compared to the competing reduction process.

Significant formation of denitration products in the presence of **HSAr[12]**–**HSAr[14]** was only observed upon addition of TEA, as indicated by TLC analysis. In comparison, almost no

conversion was observed after several hours in the absence of TEA, which suggests a process initiated by thiolate. Furthermore, significant disulfide formation was observed, too. Therefore, we propose a mechanism in accordance with initial studies by Crossley *et al*.,[12] which includes single electron transfer (SET) from thiolate to porphyrin **24** (Scheme 6). The delocalized radical anion **25** is then reduced in a sequence of elimination of nitrite to give radical **26** and abstraction of a hydrogen radical from yet unreacted thiol, so that product **27** is formed. Simultaneously, thiyl radical recombination yields the corresponding disulfide. However, more in-depth investigations of the mechanism are currently in progress.

Scheme 6 Proposed mechanism of the reduction of a nitroporphyrin in the presence of thiolate and a base.

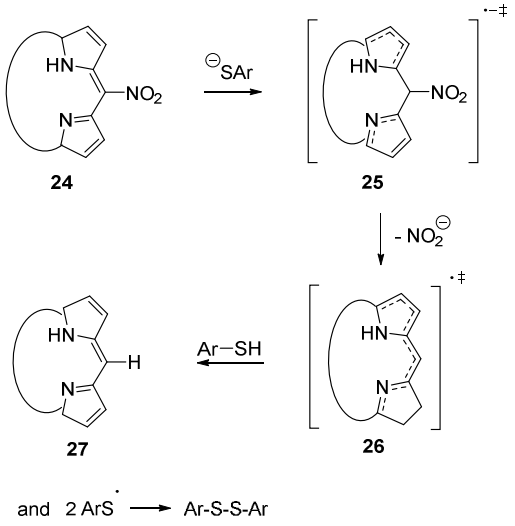

Crystallographic Studies

Highly Substituted Porphyrin Thioethers. The meso-substituted porphyrin thioethers are examples of a new class of highly substituted porphyrins. Historically, these are defined as porphyrins where *peri*-interactions of peripheral substituents result in steric strain and consequently nonplanar macrocycle conformations.[8] Single crystals suitable for X-ray crystallography were obtained for several of these dodecasubstituted tetrapyrroles, which allowed analysis of their conformational features. Likewise,

crystallography confirmed formation of the meso-tetrasubstituted compounds **2**, **9** and **10** (Fig. 1). Each of the structures revealed a high degree of nonplanarity with almost exclusive saddle distortion.[8] Table 1 allows for a comparison of the geometry of the porphyrin thioethers with the archetypical dodecasubsituted porphyrins **28** and **29**, meso-oxygen substituted porphyrin **30**, and the planar porphyrins **23** and **31**[15–19] by contrasting the average geometrical parameters of β-carbon atoms (C_b), α-carbon atoms (C_a), meso-carbon atoms (C_m), and the four internal nitrogen atoms. The deviations of macrocyclic atoms from the 24-atom mean plane of the meso-arylthio-substituted porphyrins (~0.78 Å) are comparable to **28** and **29** with only minor decreases in the deviation (0.71 and 0.62 Å, respectively).

As seen from the normal structural decomposition (NSD) analysis,[20] compounds **2**, **9** and **10** show the typical high saddle distortion (B_2u), a feature not shared by the planar counterparts **23** and **31** (Fig. 2). The overall simulated total in-plane distortion and total out-of-plane distortion (Δ_{ip} and Δ_{oop}) of the meso-thioether porphyrins **2**, **9**, and **10** are significantly higher than for compounds **23**, **28**, **29**, **30**, and **31**. There is an overall increase in the deviation of both the C_a and C_b atoms from the 24-atom mean plane. Most notably, compound **2** shows the largest deviations in ΔC_a and ΔC_b as well as average deviations of ΔC_m, $\Delta 24$, and ΔN, with only a small decrease in the core size of the porphyrin.

The pyrrole tilts of compounds **2**, **9** and **10** show much larger deviations from the 24-atom mean plane (34.9–39.3°) compared to compounds **28** and **29** (30.5 and 22.1°). This seems to be a direct result of the multifold meso-arylthio substitution. The sulfur atom forces the meso-substituent out of plane by an angle of 103.6–104.8° (C_m–S–R). Meso-sulfur-substituted porphyrins previously studied by us and Clezy *et al*. both have comparable C_m–S–R angles of 102–104.8°.[6b,21] No correlation was observed in the degree of pyrrole tilt *versus* C_m–S–R angles. Compound **2** features the highest increase in pyrrole tilt of 9°; however, it also contains the smallest C_m–S–R angles at 103.6(2)°. This increase in pyrrole tilt is most likely due to a large atom effect of the bromine atom in the packing of the structure. When compared to **30**, the C_m–O–R angle of 114.8° is larger than the C_m–S–R angle in compounds **2**, **9** and **10**. The pyrrole tilt of compound **30** (25.7°) shows a deviation from the 24-atom mean plane similar to

those of the dodecasubstituted porphyrins **28** and **29**, but much smaller tilt than for the porphyrin thioethers **2**, **9** and **10**. There is a significant decrease of the pyrrole tilts of the planar porphyrin **28** and **29** (1.6 and 4°) when compared to tetrapyrroles **2**, **9** and **10**. Overall, there are only small differences in the N–C_a–C_b, C_a–N–C_a, C_a–C_m–C_a, and C_a–C_b–C_b angles of porphyrin thioethers **2**, **9** and **10** when compared to those of the dodecasubstituted porphyrins **28** and **29**. The N–C_a–C_m angle shows a decreased size of 119.9–120.6° for **2**, **9** and **10** compared to 122.5 and 124.1° for **28** and **29**, while the C_m–C_a–C_b angles show a minor increase with 130.3–130.9° compared to 129.0 and 127.1°, respectively. In conclusion, **9** and **10** have traits similar to the archetypical dodecasubstituted porphyrins **28** and **29** with regards to distortion mode, increased pyrrole tilt, atom deviations from the 24-atom mean plane, N–C_a–C_b angles, and N–C_a bond lengths. However, specific features are clearly reminiscent of previously studied sulfur porphyrins, such as the C_m–S–R angles.

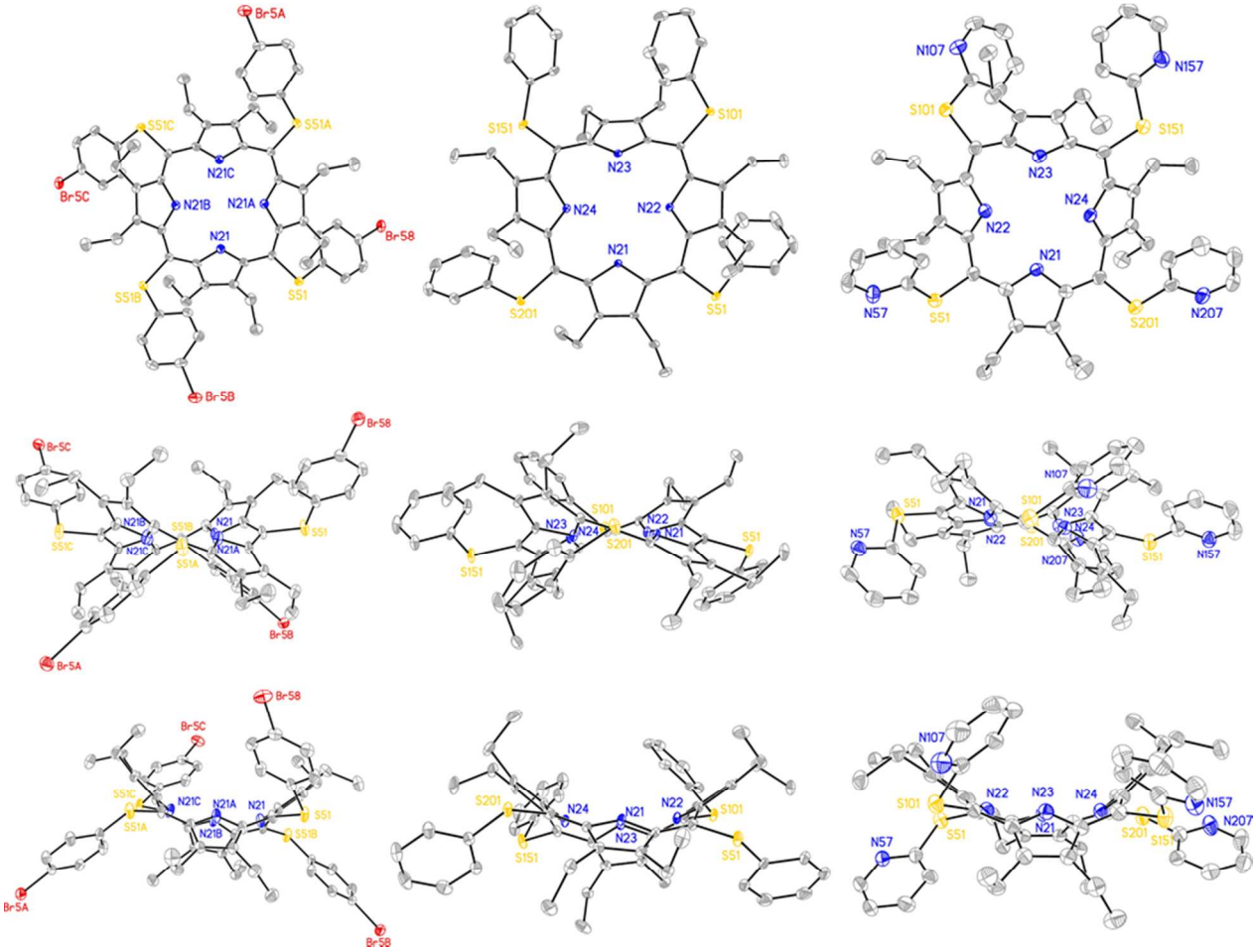

Figure 1. Top and two side views of the crystal structures of 2 (left), 9 (middle)

and 10 (right). Hydrogen atoms and minor disorder have been omitted for clarity, thermal ellipsoids indicate 50% probability.

Table 1. Averaged geometrical parameters for bond lengths, angles, core conformation and atom displacements of the porphyrin thioethers 2, 9 and 10 and comparative examples.

	2	**9**	**10**	**28•DCM**[15]	**28•EtOH**[15]	**29**[16]	**30**[17]	**23**[18]	**31**[19]
Bond lengths (Å):									
N–C_a	1.364(4)	1.368(3)	1.370(7)	1.363	1.369	1.366	1.369	1.366	1.369
C_a–C_b	1.447(4)	1.453(3)	1.453(7)	1.480	1.457	1.457	1.444	1.450	1.442
C_a–C_m	1.413(4)	1.411(3)	1.411(7)	1.424	1.411	1.412	1.364	1.392	1.399
C_b–C_b	1.381(5)	1.371(3)	1.375(7)	1.361	1.367	1.387	1.354	1.363	1.351
Bond angles (°):									
N–C_a–C_m	119.9(3)	120.6(2)	120.6(5)	120.7	122.5	124.1	121.2	125.0	126.2
N–C_a–C_b	108.9(3)	108.8(2)	108.7(4)	111.4	108.26	108.7	110.1	109.3	108.8
Ca–N–C_a	108.4(3)	108.2(2)	108.5(4)	105.5	108.84	109.0	106.1	107.7	107.7
Ca–C_m–C_a	123.1(3)	124.1(2)	124.2(5)	120.7	124.0	123.0	125.9	127.6	125.6
C_a–C_b–C_b	106.6(3)	106.9(2)	106.9(5)	105.7	107.1	106.8	106.8	106.9	107.5
C_m–C_a–C_b	130.9(3)	130.3(2)	130.3(5)	127.9	129.0	127.1	127.9	125.7	125.1
C_m–S/O–C_{Ph}	103.6(2)	103.8(1)	104.3(3)	-	-	-	114.8	-	-
Pyrrole tilt	39.3(9)	34.9(6)	34.7(9)	44.1	30.5	22.1	25.7	1.634	4.032
Structural parameters (Å):									
Δ_{ip}[a]	1.01	0.74	0.79	1.02	0.52	0.68	0.65	0.23	0.20
Δ_{oop}[b]	4.23	3.83	3.80	4.29	3.46	3.01	2.29	0.11	0.26
Core size[c]	2.90	2.92	2.93	3.01	2.91	2.91	2.67	2.92	2.92
Δ24[d]	0.78	0.79	0.78	0.84	0.71	0.62	0.47	0.03	0.07
ΔN[e]	0.05	0.06	0.07	0.19	0.07	0.14	0.01	0.03	0.09
ΔC_m[f]	0.15	0.20	0.10	0.60	0.04	0.07	0.79	0.02	0.03
ΔC_a[g]	0.52	0.46	0.46	0.23	0.42	0.36	0.46	0.01	0.03
ΔC_b[h]	1.41	1.26	1.27	1.37	1.16	0.99	0.39	0.03	0.06

[a] Simulated total in-plane distortion. [b] Simulated total out-of-plane distortion. [c] Average distance between adjacent pyrrole nitrogen atoms. [d] Average deviation from the least-squares plane of the 24-macrocycle atoms. [e] Simulated displacement of the four internal nitrogen atoms from the 24-atom mean plane. [f] Average deviation of the meso-carbon atoms from the 24-atom mean plane. [g] Average deviation of the α-carbon atoms from the 24-atom mean plane. [h] Average deviation of the β-carbon atoms from the 24-atom mean plane.

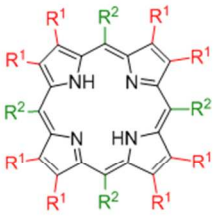

Entry	M	R^1	R^2	Compound
1[a]	2H	Et	Ph	**28**
2	2H	Ph	Ph	**29**
3	Ni(II)	Et	Bz	**30**
4	2H	H	Ph	**31**

[a] Two known crystal forms; DCM or EtOH solvate.[15]

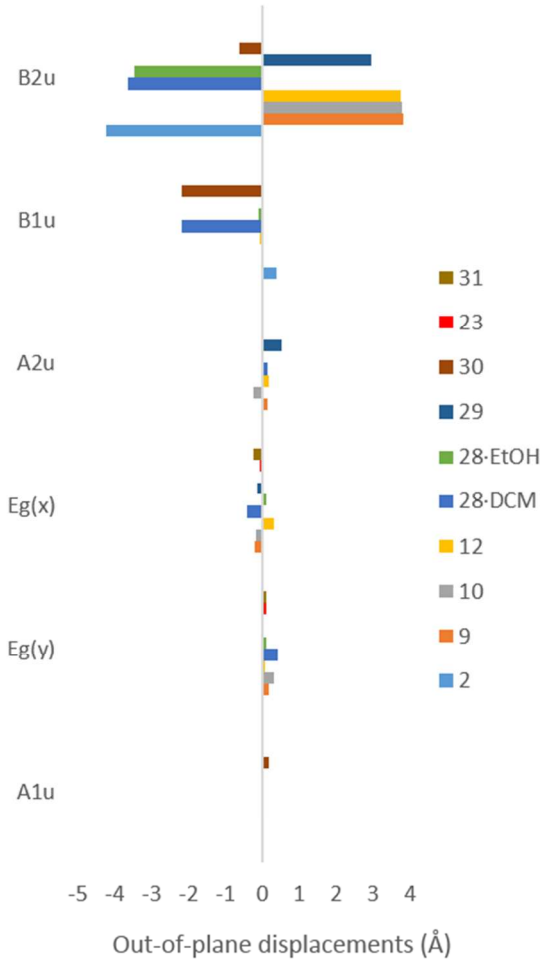

Figure 2. Normal structural decomposition (NSD) analysis of the X-ray crystallographic structures of 2, 9, 10 and selected other highly substituted porphyrins. Distortions of 23 and 31 are included for comparison.

Meso-(nitro)$_x$-OEPs. The denitration reactions described above gave access to several new structures of meso-nitro-substituted octaethylporphyrins (OEPs), which – together with structures available from the literature – allowed for a comparative analysis of the structural features of OEPs with different numbers and regiochemical arrangements of meso-nitro units. Previous studies featuring meso-nitro and β-nitro groups include, for example Barkigia *et al.* study on iron(III) porphyrin complexes presenting a variety of ligands with a varying degree of distortion.[22] However, there is currently no example of a comparative structural study focusing on the effects of a varying degree of meso-nitro substitution.

Comparison of the saddled distortion mode of the meso-(nitro)$_x$-OEPs with **23** (Fig. 3) reveals that the latter has no visible distortion while **22** shows only a small contribution, indicating minor saddle distortion. A notable increase in the B_{2u} mode of compound **20** suggests that multifold nitro substitution results in increased distortion. However, when this is compared to tetrapyrrole **21**, the influence of regiochemical placement of the nitro substituents proves to be of importance as a 'flattening' of the porphyrin ring is noted. Compound **32**, previously synthesized but crystallized here for comparison, displays the most notable change, as there is no more contribution to the B_{2u} mode with the largest contribution being in the ruffled distortion mode (B_{1u}). Ultimately, it can be seen that compound **1**, carrying four nitro groups, shows the largest contribution to the B_{2u} mode, again suggesting that higher meso-nitro substitution distorts the porphyrin ring to a much larger degree. This is clearly shown in Fig. 4, where compound **20** has a larger visual distortion as compared to **21** and **32**, which are notably more planar. Comparing the Δ_{oop} of compounds **1**, **20**, **21**, **22**, and **32** reveals that porphyrins **1** and **20** have the highest values while at the same time, their Δ_{ip} are the smallest. This is also evidenced in Table 2 with the structural parameters showing trends accordingly. There is a small but notable elongation of the N–C_a bond length in the order **22** < **20** < **21** < **32**, followed by a decreased bond length in compound **1**. The C_b–C_b and C_a–C_b bonds both show moderate increase in length in the orders **22** < **20** = **21** < **32** < **1** and **22** < **1** < **21** < **20** < **32**, while the C_a–C_m bond lengths decrease in the sequence **22** < **20** = **32** < **21** with a subtle increase in **1**. Analysis of the bond angles reveals a similar trend; While the N–C_a–C_b, C_a–N–C_a, and C_a–C_b–C_b angles undergo little or no change, the N–C_a–C_m

angles show a decrease of about 4° in the order **22** < **20** = **21** < **32** < **1**. The C_a—C_m—C_a bond angles ascend in the sequence **22** < **20** < **21** < **32**, with compound **1** displaying angles similar to **22**. The C_m—C_a—C_b angles show a general increase (**22** < **20** < **21** < **32** < **1**), with the pyrrole tilts rising in the order **22** = **21** < **32** < **20** < **1**. This trend is followed for the atom displacements of Δ24 and ΔC_a; however, ΔN shows a trend of **22** < **21** < **32** < **20** < **1**, ΔC_m of **21** < **22** < **32** < **1** < **20** and ΔC_b of **32** < **22** < **22** < **20** < **1**. The core size shows a slight elongation (**22** < **21** < **32** < **20**) with a sharp constriction in compound **1**. In conclusion, the macrocyclic distortion of meso-(nitro)$_x$-OEPs significantly depends on the extent and pattern of nitro substitution.

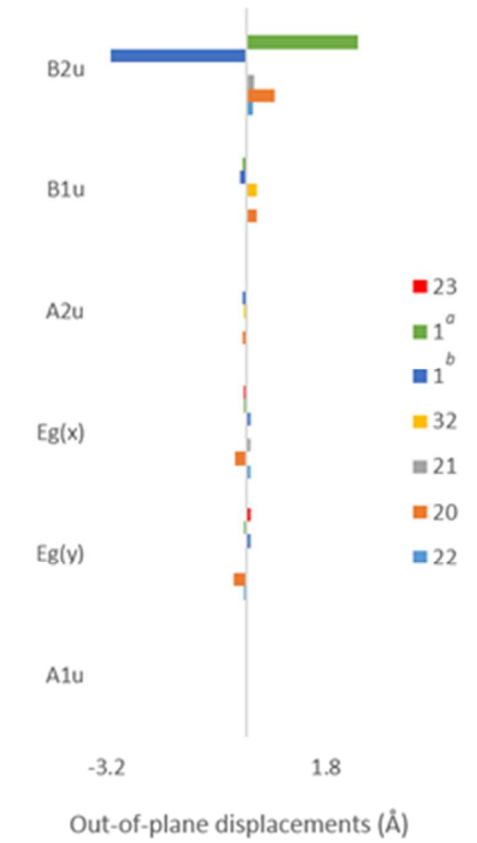

[a] Data collection at 130 K. [b] Data collection at 283–303 K.

Figure 3. NSD of the X-ray crystallographic structures of meso-(nitro)$_x$-OEPs. Distortions of 23 are included for comparison.

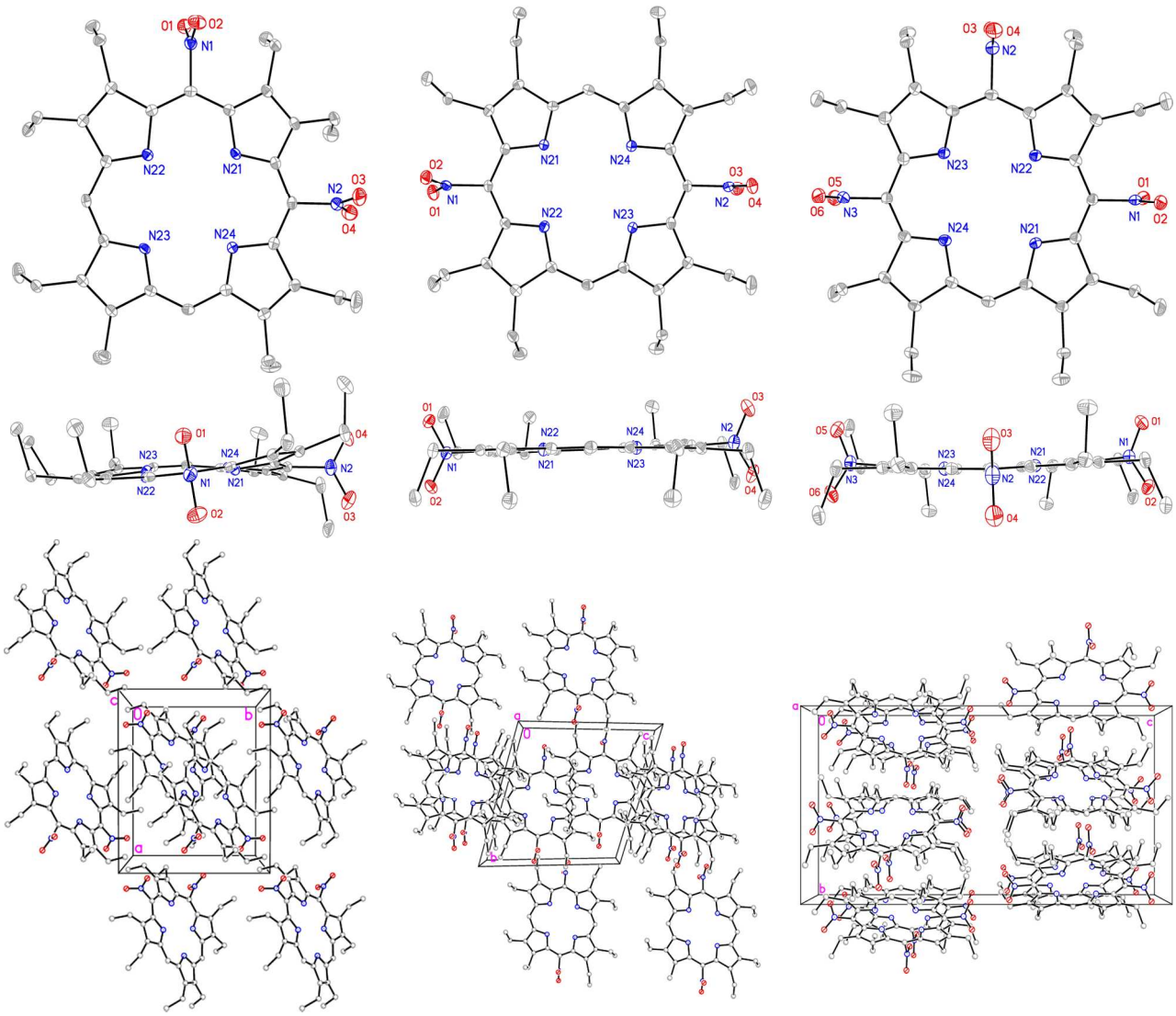

Figure 4. Top, side and packing views of the crystal structures of 20 (left), 21 (middle) and 32 (right). Hydrogen atoms have been omitted for clarity, thermal ellipsoids indicate 50% probability.

Table 2. Averaged geometrical parameters for bond lengths, angles, core conformation and atom displacements of meso-(nitro)$_x$-OEPs.

	22[3b]	**20**	**21**	**32**	**1**[3a]	**1**[3c]	**18**
Bond lengths (Å):							
N—C_a	1.364	1.366(5)	1.367(9)	1.368(3)	1.362	1.363	1.378(4)
C_a—C_b	1.449	1.454(5)	1.451(7)	1.456(3)	1.450	1.458	1.450(5)
C_a—C_m	1.396	1.394(5)	1.393(7)	1.394(3)	1.399	1.397	1.380(4)
C_b—C_b	1.364	1.365(5)	1.365(7)	1.366(3)	1.375	1.368	1.361(5)

Bond angles (°):							
N–C_a–C_m	124.2	123.6(2)	123.6(3)	123.0(2)	120.5	121.0	122.9(2)
N–C_a–C_b	109.7	109.5(2)	109.5(4)	109.5(2)	109.4	109.6	111.1(2)
C_a–N–C_a	107.3	107.5(3)	107.5(3)	107.5(2)	107.9	107.4	104.7(3)
C_a–C_m–C_a	128.8	129.5(2)	130.1(4)	131.5(2)	128.9	130.5	125.8(1)
C_a–C_b–C_b	106.7	106.7(2)	106.8(4)	106.8(2)	106.6	106.5	106.4(2)
C_m–C_a–C_b	126.1	126.8(1)	126.9(4)	127.5(2)	129.8	129.2	125.6(1)
Pyrrole tilt	1.7	7.1(5)	1.7(9)	2.7(7)	25.5	20.5	17.3(8)
Structural parameters (Å):							
Δ_{ip}[a]	0.34	0.30	0.50	0.46	0.39	0.13	0.23
Δ_{oop}[b]	0.17	0.80	0.19	0.24	3.11	2.52	0.11
Core size[c]	2.93	2.94	2.94	2.95	2.91	2.93	2.75
Δ24[d]	0.04	0.16	0.04	0.05	0.64	0.52	0.31
ΔN[e]	0.02	0.07	0.01	0.03	0.10	0.08	0.02
ΔC_m[f]	0.03	0.11	0.02	0.08	0.05	0.03	0.53
ΔC_a[g]	0.02	0.09	0.02	0.04	0.40	0.32	0.31
ΔC_b[h]	0.04	0.21	0.06	0.03	1.02	0.83	0.22

[a] Simulated total in-plane distortion. [b] Simulated total out-of-plane distortion. [c] Average distance between adjacent pyrrole nitrogen atoms. [d] Average deviation from the least-squares plane of the 24-macrocycle atoms. [e] Simulated displacement of the four internal nitrogen atoms from the 24-atom mean plane. [f] Average deviation of the meso-carbon atoms from the 24-atom mean plane. [g] Average deviation of the α-carbon atoms from the 24-atom mean plane. [h] Average deviation of the β-carbon atoms from the 24-atom mean plane.

Previous studies into nitro-substituted OEP metal complexes have elucidated the structures of several examples of Fe(III) penta-coordinated complexes (Fig. 5). Iron(III) porphyrin **33**[8] shows similar displacement as the corresponding free base with the Fe(III) center sitting above the 24-atom mean plane. Complexes **34**,[3e] **35**,[23] **36**,[3e] and **37**[3e] have been reported as planar dimers with both rings joined by metal peroxide bridges. Tetrapyrrole **38**[24] shows a significant saddle distortion similar to the free base counterpart. Additionally, the structures of several examples of tetra- and penta-coordinated Zn(II) complexes have been determined. Compounds **39**,[3b] **40**,[3b] and **41**[3a]

show planarity similar to the corresponding free bases. Interestingly, the structure of **42**[3d] demonstrated to be polymeric with highly distorted porphyrin moieties bending and rotating to accommodate a nitro group, which coordinates to the Zn(II) center of one porphyrin, thus forming a continuous chain.

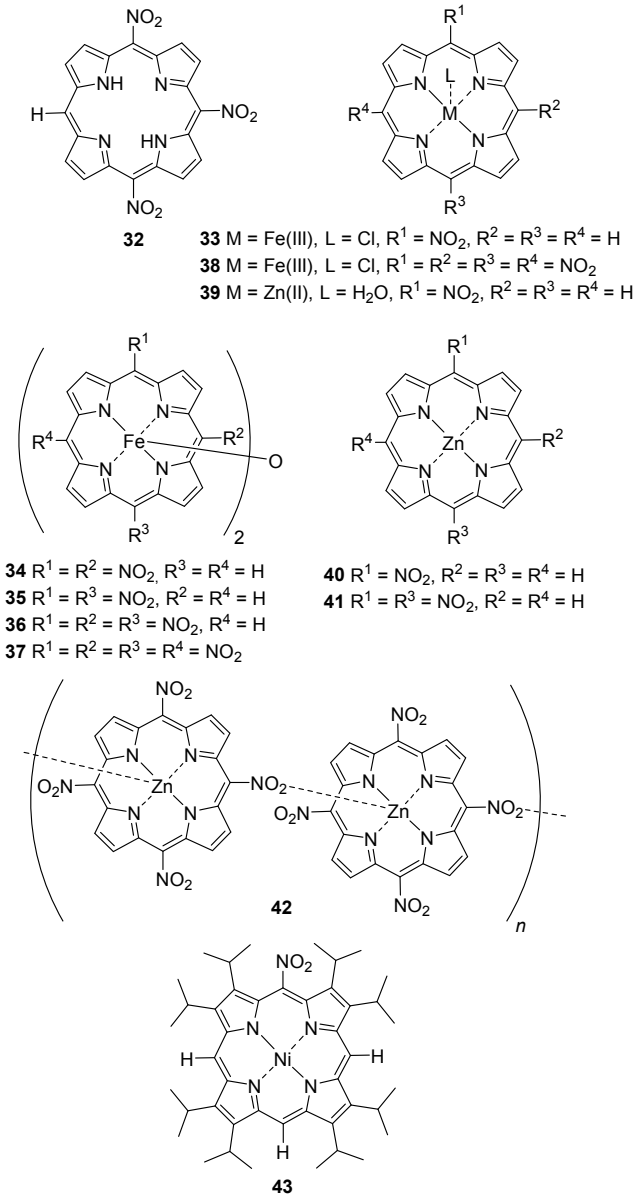

Figure 5. Selection of previously synthesized nitro-substituted porphyrin complexes.

In this work, the structure of the nickel(II) complex **18** was determined as well (Fig. 6).

As expected, when compared to free base **20**, there is an increase in the N–C_a bond lengths and a decrease in the C_a–C_m bond lengths. An increase is also noticed in the N–C_a–C_b bond angles, along with notably decreased C_a–N–C_a and C_a–C_m–C_a angles. An increase in the Δ24, ΔC_m, and ΔC_a displacements coupled with the increased pyrrole tilt angles indicates the ruffled distortion mode. In comparison, the two tetra-coordinated complexes **17**[3c] and a corresponding isopropyl-substituted Ni(II) porphyrin (**43**)[25] show similar C_a–C_m–C_a angles at 125.0 and 126.4°, which also applies to the C_a–N–C_a angle (104°). There is a similar relationship with a decrease in the core size from **18** (2.746 (7)°) to **17** (2.717°). This trend is similar to that seen with the free base counterparts and confirms related studies on the conformational effects in meso-substituted porphyrin regioisomers.[26]

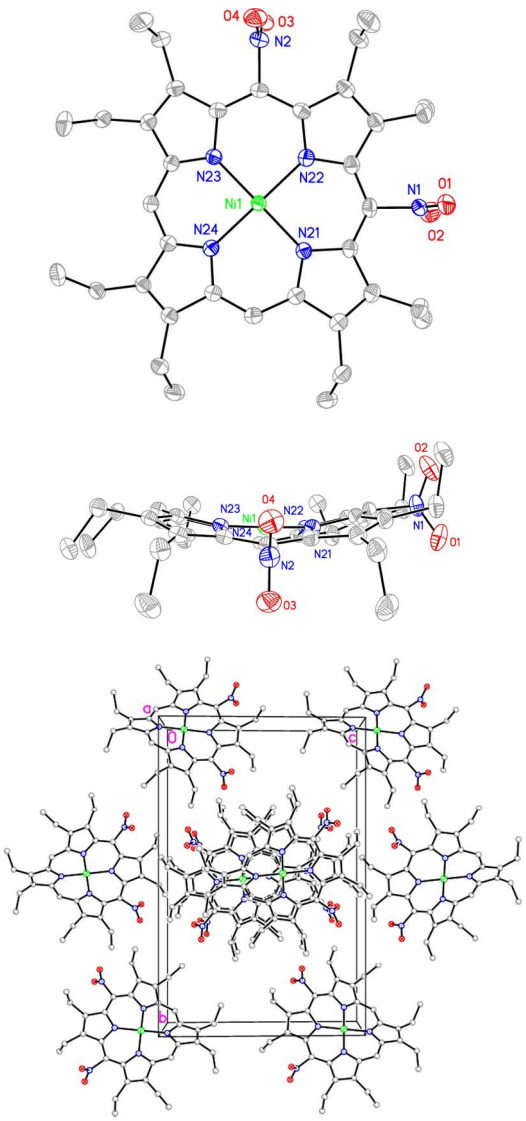

Figure 6. Side view of the crystal structures of 18: top (top), side (middle) and packing (bottom). Hydrogen atoms have been omitted for clarity, thermal ellipsoids indicate 50% probability.

CONCLUSIONS

In summary, we synthesized a range of highly substituted, nonplanar porphyrin thioethers from one precursor (**1**) in moderate to good yield, which also proved to be insensitive to air and moisture, thus allowing for convenient syntheses without protective atmosphere. The reactions involved a S_NAr method that was applied using both electron-rich and -poor, as well as bulky aromatic thiolate nucleophiles. This method

may be used as a versatile tool for the linkage of functional groups or chromophores to porphyrin scaffolds with minimal synthetic effort. Additionally, a methodology for the stepwise desubstitution of **1** was developed, which may be expanded to other nitroaromatic compounds in the future.

Over the course of this study we have determined the structure of three new meso-arylthio-substituted tetrapyrroles (**2**, **9** and **10**) as the first examples of a new class of highly substituted porphyrins. These compounds exhibit specific features that are reminiscent of previously studied porphyrin thioethers, such as the C_m–S–R angles. However, they also possess the structural features of highly substituted porphyrins, such as increased pyrrole tilts and atom deviations from the 24-atom mean plane. Additionally, we have reported the first complete study into the effects of an incremental increase of meso-nitro substitution on highly substituted porphyrins, elucidated macrocyclic deviations based on the number and pattern of nitro substituents. This was accompanied by thorough structural analysis of **18** and comparison to similar complexes and its free base counterpart.

EXPERIMENTAL

General Experimental Methods. Analytical thin-layer chromatography (TLC) was performed using sheets precoated with silica gel to a depth of 0.2 mm or aluminum oxide plates, both impregnated with fluorescence indicator F_{254}. Visualization was accomplished with UV lamp. Column chromatography was carried out using silica gel 60 (230–400 mesh) or aluminum oxide (neutral, activated with 6% H_2O, Brockman Grade III. Mass spectrometry was performed using ESI or MALDI ionization methods with a TOF mass analyzer. UV-Vis absorption measurements were performed in DCM or toluene as solvent. Melting points are uncorrected. ^{1}H, ^{13}C {^{1}H} and ^{19}F NMR spectra were recorded at 400.13 MHz, 100.61 MHz and 376.59 MHz. All NMR experiments were performed at 25 °C. Resonances δ are given in ppm units and referenced to the deuterium peak in the NMR solvent, $CDCl_3$ (δ_H = 7.26 ppm, δ_C = 77.2 ppm). Signal multiplicities are abbreviated as follows: Singlet = s, multiplet = m. Photophysical measurements were carried out in DCM or toluene as solvent.

In some NMR spectra of the new 2,3,7,8,12,13,17,18-octaethyl-5,10,15,20-tetrasubstituted porphyrin thioethers, the signals corresponding to the β-ethyl groups are broad. This is in accordance with conformational studies by Medforth *et al.* on decaalkylporphyrins.[27] Presumably, the highly substituted products exist as a mixture of atropisomers in solution, particularly in the case of unsymmetrical meso-substituents as in **12**, causing signal broadening due to different interactions between β-ethyl groups and meso-substituents. Opposed to this, the introduction of bulky substituents such as anthracenyl and mesityl groups resulted in a "locking" of the conformation and clearer signals for the β-ethyl groups. However, variable temperature NMR experiments could not be performed due to the low solubility of the compounds in appropriate solvents, such as DMSO-d_6, or THF-d_8. Missing signals corresponding to the inner protons as observed in most ^{1}H NMR spectra have been reported previously, too.[28]

Materials. 9-Anthracenethiol (**HSAr^4**),[29] H_2OETNP (**1**),[28] its Ni(II) complex **17**[3c], and **32**[28] were prepared according to the literature and gave satisfactory analytical data. 9-Phenanthrenthiol (**HSAr^{10}**)[30] was prepared similar to **HSAr^4**.[29] The synthesis of **18** has been reported previously, but full characterization was unavailable.[31]

Substitution Reactions

Reaction of H_2OETNP with 4-bromobenzenethiol in absence of TEA. In a 50 mL round bottom flask fitted with a reflux condenser, compound **1** (75 mg, 0.11 mmol, 1 equiv.) and 4-bromobenzenethiol (**HSAr^1**, 1.05 mmol, 198 mg, 10 equiv.) were dissolved in 10 mL of chloroform and heated to 61 °C for 19 h. Upon consumption of the starting material, as indicated by TLC analysis, the solvent was removed *in vacuo* and column chromatography was performed. The second fraction of the first column chromatography (SiO_2, hexane:DCM, 2:1, v/v) yielded an inseparable mixture of the isomers **4** and **5** as a purple solid (15 mg of a 3:2 mixture, combined yield 16%) after elution of less polar side products, removal of the solvent and recrystallization by slow diffusion from DCM and methanol. The column was flushed with ethyl acetate, the solvent was removed and two more chromatographic purification steps of this fraction were performed: The first chromatography (SiO_2, hexane + 1% TEA) gave **2** (60 mg,

53%) as the first major fraction upon removal of the solvent. Subsequently, the column was flushed with ethyl acetate, the solvent was removed and this fraction was purified by chromatography (Al_2O_3, hexane:DCM, 50:1–1:1, v/v) to give **3** (40 mg, 30%) as the major component upon removal of the solvent. Compound **2** was obtained as green crystals after recrystallized by slow evaporation (acetone:water, 10:1, v/v).

5,10,15,20-Tetrakis[(4-bromophenyl)thio]-2,3,7,8,12,13,17,18-octaethylporphyrin 2: mp 115–120 °C dec. R_f 0.78 (SiO_2, hexane:ethyl acetate, 10:1, v/v). ^{1}H NMR (400.13 MHz, $CDCl_3$, δ) 0.96–1.90 (m, 24H), 2.60–3.67 (m, 16H), 6.74–6.95 (m, 8H), 7.10–7.25 (m, 8H). ^{13}C {^{1}H} NMR (100.61 MHz, $CDCl_3$, δ) 16.7, 20.3, 119.2, 127.5, 132.1, 141.9. UV (DCM) λ_{max} (log ε) 488 (5.01), 581 (3.84), 639 (3.83), 743 nm (3.75). HRMS–MALDI (*m/z*): M^+ calcd for $C_{60}H_{58}Br_4N_4S_4$, 1278.0278; found, 1278.0283. MS–MALDI *m/z* (% relative intensity, ion): 907 (100), 531 (43, M − 4SAr + H), 685 (30, M − 3SAr).

5,10,15-Tris[(4-bromophenyl)thio]-2,3,7,8,12,13,17,18-octaethylporphyrin 3: mp 87–90 °C dec. R_f 0.64 (Al_2O_3, hexane:DCM, 2:1, v/v). ^{1}H NMR (400.13 MHz, $CDCl_3$, δ) 0.97–1.19 (m, 12H), 1.42–1.53 (m, 12H), 2.70–3.53 (m, 8H), 2.54–3.63 (m, 4H), 3.64–4.04 (m, 4H), 6.65–6.75 (m, 4H), 6.79–6.98 (m, 2H), 7.04–7.10 (m, 2H), 7.12–7.18 (m, 4H), 8.92 (s, 1H). ^{13}C {^{1}H} NMR (100.61 MHz, $CDCl_3$. δ) 17.0, 17.3, 17.7, 19.4, 20.3, 20.4, 22.1, 29.6, 118.8, 119.3, 127.5, 132.0, 132.1, 142.5. UV (DCM) λ_{max} (log ε) 469 (5.01), 567 (3.92), 617 (3.94), 700 nm (3.57). HRMS–MALDI (*m/z*): $[M + H]^+$ calcd for $C_{54}H_{56}Br_3N_4S_3$, 1093.1212; found, 1093.1216. MS–MALDI *m/z* (% relative intensity, ion): 503 (100), 531 (93, M − 3SAr), 719 (53, M − 2SAr + H).

5,10-Bis[(4-bromophenyl)thio]-2,3,7,8,12,13,17,18-octaethylporphyrin 4 and 5,15-bis[(4-bromophenyl)thio]-2,3,7,8,12,13,17,18-octaethylporphyrin 5: HRMS–ESI (*m/z*): $[M + H]^+$ calcd for $C_{48}H_{53}Br_2N_4S_4$, 909.2058; found, 909.2055.

5,10,15,20-Tetrakis[(4-bromophenyl)thio]-2,3,7,8,12,13,17,18-octaethylporphyrin (2) (Synthesis in the presence of TEA): In a sample tube, porphyrin **1** (30 mg, 42 *μ*mol, 1 equiv.) and 4-bromobenzenethiol (**HSAR[1]**, 35 mg, 0.18 mmol, 4.4 equiv.) were dissolved in chloroform (2 mL) and TEA (3 drops) was added. The color changed to dark red within 10 min and the crude product was chromatographed on silica (hexane:ethyl acetate, 40:1–10:1, v/v). A green band was collected to give the green

solid **3** (<10%) upon removal of the solvent while the second fraction (dark red band) yielded **2** (39 mg, 73%) as a green solid after evaporation of the solvent.

2,3,7,8,12,13,17,18-Octaethyl-5,10,15-tris(mesitylthio)porphyrin 6: Compound **1** (25 mg, 35 μmol, 1 equiv.), 2,4,6-trimethylthiophenol (**HSAr**^{2}, 24 mg, 0.15 mmol, 4.4 equiv.) and TEA (3 drops) were reacted at 25 °C in chloroform (5 mL) until completion, as indicated by TLC analysis. The solvent was removed *in vacuo* and column chromatography (SiO_2, hexane:ethyl acetate, 75:1–0:1, v/v) was performed. After the removal of less polar side products, **6** was obtained as a green solid (16 mg, 40%) upon evaporation of the solvent. mp 54–57 °C dec. R_f 0.21 (SiO_2, hexane:ethyl acetate, 4:1, v/v). ^{1}H NMR (400.13 MHz, $CDCl_3$, δ) 0.68–0.72 (m, 6H), 1.47–1.50 (m, 6H), 1.60–1.63 (m, 12H), 1.95–1.98 (m, 18H), 2.25–2.28 (m, 9H), 2.81–2.82 (m, 4H), 3.01–3.15 (m, 4H), 3.32–3.34 (m, 4H), 3.64–3.66 (m, 4H), 6.70 (s, 6H), 7.88 (s, 1H). ^{13}C {^{1}H} NMR (100.61 MHz, $CDCl_3$, δ) 16.2, 16.5, 16.8, 17.3, 18.7, 19.0, 19.1, 21.0, 21.2, 21.4, 21.7, 22.0, 29.6, 32.1, 90.4, 129.8 (x2), 133.4, 134.0, 136.3, 136.8, 138.7, 138.2, 143.5, 143.7. UV (DCM) λ_{max} (log ε) 470 (5.07), 592 (4.01), 632 (4.25), 718 nm (3.87). HRMS–MALDI (*m/z*): $[M + H]^+$ calcd for $C_{63}H_{77}N_4S_3$, 985.5310; found, 985.5313.

5,10,15-Tris(anilin-4-ylthio)-2,3,7,8,12,13,17,18-octaethylporphyrin 7: Compound **1** (30 mg, 42 μmol, 1 equiv.) and 4-aminobenzenethiol (**HSAr**^{3}, 41 mg, 0.33 mmol, 7.8 equiv.) were dissolved in 6 mL of chloroform and TEA (3 drops) was added. The resulting solution was stirred at 25 °C for 20 min. After removal of the solvent at reduced pressure, the residue was purified by column chromatography (SiO_2, hexane:ethyl acetate, 75:1–0:1, v/v) and compound **7** was obtained as a green solid (15 mg, 40%) upon removal of the solvent. mp 98–102 °C dec. R_f 0.13 (SiO_2, ethyl acetate). ^{1}H NMR (400.13 MHz, $CDCl_3$, δ) 0.96–1.01 (m, 12H), 1.47–1.55 (m, 12H), 3.00–4.00 (m, 22H), 6.29-6.36 (m, 2H), 6.36-6.44 (m, 2H), 6.52-6.65 (m, 2H), 6.70-6.85 (m, 2H), 8.63 (s, 1H). ^{13}C {^{1}H} NMR (100.61 MHz, $CDCl_3$, δ) 16.1, 17.1, 17.4, 17.6, 19.3, 22.1, 27.1, 115.1, 116.1 (x2), 128.4, 128.7, 134.1, 144.2, 144.6. UV (DCM) λ_{max} (log ε) 478 (4.23), 626 (3.32), 755 nm (3.30). HRMS–MALDI (*m/z*): $[M + H]^+$ calcd for $C_{54}H_{62}N_7S_3$, 904.4229; found, 904.4254.

5,10,15-Tris(anthracen-9-ylthio)-2,3,7,8,12,13,17,18-octaethylporphyrin 8: Compound **1** (40 mg, 56 μmol, 1 equiv.), 9-anthracenethiol (**HSAr[4]**, 103 mg, 0.49 mmol, 8.8 equiv.) and TEA (3 drops) were reacted at 25 °C in chloroform (8 mL) until completion, as indicated by TLC analysis. After removal of the solvent *in vacuo*, column chromatography was performed (SiO_2, hexane:ethyl acetate, 75:1–0:1, v/v) to remove less polar side products. The first major fraction was collected, the solvent was removed and recrystallization by slow diffusion from DCM and petroleum ether gave **8** as a green solid (23 mg, 35%). mp 138–142 °C dec. R_f 0.39 (SiO_2, ethyl acetate). ^{1}H NMR (400.13 MHz, $CDCl_3$, δ) 0.56–0.74 (m, 12H), 1.20–1.35 (m, 6H), 1.36–1.53 (m, 6H), 2.41–2.57 (m, 4H), 2.71–2.87 (m, 4H), 2.99–3.13 (m, 4H), 3.19–3.38 (m, 4H), 6.70–6.93 (m, 2H), 6.99–7.11 (m, 4H), 7.26–7.35 (m, 6H), 7.60 (s, 1H), 7.87–8.01 (m, 8H), 8.01–8.12 (m, 2H), 8.28–8.43 (m, 7H). ^{13}C {^{1}H} NMR (100.61 MHz, $CDCl_3$, δ) 16.4 (C*H$_3$*), 16.6 (x2), 17.0, 18.9, 19.2, 21.1, 22.6, 53.6, 91.7, 125.2, 125.6, 126.1, 126.3, 128.0, 128.7, 128.9, 130.3, 130.9, 131.6 (x2), 131.8, 132.0, 132.2, 142.6. UV (toluene) λ_{max} (log ε) 417 (4.77), 489 (4.67), 678 (3.96), 753 nm (3.88). HRMS–MALDI (*m/z*): $[M + H]^+$ calcd for $C_{78}H_{71}N_4S_3$, 1159.4841; found, 1159.4828. MS–MALDI *m/z* (% relative intensity, ion): 503 (100), 531 (81, M − 3SAr), 741 (65, M − 2SAr + H), 950 (12, M − SAr).

2,3,7,8,12,13,17,18-Octaethyl-5,10,15,20-tetrakis(phenylthio)porphyrin 9: A sample tube was charged with H_2OETNP (**1**, 30 mg, 42 μmol, 1 equiv.) and 6 mL of chloroform. Upon addition of thiophenol (**HSAr[5]**, 20 mg, 0.19 mmol, 4.4 equiv.) and TEA (3 drops), the mixture was allowed to react at 25 °C for 5 min. The solvent was removed *in vacuo* and the crude product was purified by column chromatography (SiO_2, hexane:ethyl acetate, 75:1–0:1, v/v). After elution of less polar side products, the title compound was obtained as a green solid (35 mg, 86%) upon evaporation of the solvent. Recrystallization by slow evaporation (hexane:ethyl acetate, 10:1, v/v) yielded green crystals. mp 209–212 °C dec. R_f 0.48 (SiO_2, hexane:ethyl acetate, 2:1, v/v). ^{1}H NMR (400.13 MHz, $CDCl_3$, δ) 0.93–1.32 (m, 24H), 2.85–3.53 (m, 16H), 6.89–7.16 (m, 20H). ^{13}C {^{1}H} NMR (100.61 MHz, $CDCl_3$, δ) 16.8, 20.2, 125.3, 126.0, 129.1, 142.4. UV (DCM) λ_{max} (log ε) 487 (4.82), 584 (3.63), 639 (3.66), 748 nm (3.54). HRMS–MALDI (*m/z*): [M +

H]$^+$ calcd for $C_{60}H_{63}N_4S_4$, 967.3936; found, 967.3948. MS–MALDI *m/z* (% relative intensity, ion): 611 (100), 857 (10, M − SAr).

2,3,7,8,12,13,17,18-Octaethyl-5,10,15,20-tetrakis(pyridine-2-ylthio)porphyrin 10: Tetrapyrrole **1** (10 mg, 14 μmol, 1 equiv.), 2-mercaptopyridine (**HSAr**[6], 7.2 mg, 65 μmol, 4.4 equiv.) and TEA (3 drops) were reacted at 25 °C in chloroform until completion, as indicated by TLC analysis. The solvent was removed *in vacuo* and column chromatography (SiO_2, ethyl acetate) was performed to remove less polar side products. The title compound was obtained as a green solid (9.5 mg, 65%) after recrystallization by slow evaporation (acetone:water, 10:1, v/v). mp 205–210 °C dec. R_f 0.13 (SiO_2, ethyl acetate). ^{1}H NMR (400.13 MHz, $CDCl_3$, δ) 0.94–1.21 (m, 12H), 1.35–1.76 (m, 12H), 2.72–3.67 (m, 16H), 6.02–6.67 (m, 4H), 6.94–7.17 (m, 8H), 8.43–8.58 (m, 4H). ^{13}C {^{1}H} NMR (100.61 MHz, $CDCl_3$, δ) 16.5, 20.2, 120.0, 120.8, 136.8, 142.6, 149.6, 165.7. UV (DCM) λ_{max} (log ε) 482 (5.06), 579 (3.90), 635 (3.83), 744 nm (3.52). HRMS–MALDI (*m/z*): [M + H]$^+$ calcd for $C_{56}H_{59}N_8S_4$, 971.3740; found, 971.3713. MS–MALDI *m/z* (% relative intensity, ion): 529 (100, M − 4SAr – H), 530 (86, M − 4SAr), 640 (38, M − 3SAr), 751 (4, M − 2SAr + H).

2,3,7,8,12,13,17,18-Octaethyl-5,10,15,20-tetrakis[(4-isopropylphenyl)thio]porphyrin 11: 4-Isopropylbenzenethiol (**HSAr**[7], 28 mg, 0.19 mmol, 4.4 equiv.) was added to a solution of porphyrin **1** (30 mg, 42 μmol, 1 equiv.) in 4 mL of chloroform and TEA (3 drops) was added. The reaction mixture was stirred at 25 °C for 5 min, the color changed from brown to dark red and the crude product was purified by column chromatography (SiO_2, hexane:ethyl acetate, 75:1–2:1, v/v). After separation of less polar side products, **11** was obtained as a green solid (30 mg, 63%) upon removal of the solvent. mp 107–110 °C dec. R_f 0.31 (SiO_2, hexane:ethyl acetate, 8:1, v/v). ^{1}H NMR (400.13 MHz, $CDCl_3$, δ) 0.93–1.25 (m, 24H), 1.14–1.20 (m, 24H), 2.72–2.85 (m, 4H), 2.72–3.46 (m, 16H), 6.81–6.98 (m, 16H). ^{13}C {^{1}H} NMR (100.61 MHz, $CDCl_3$, δ) 16.8, 20.1, 24.1, 33.7, 126.4, 126.8, 127.1,133.4, 136.8, 139.2, 145.9. UV (DCM) λ_{max} (log ε) 490 (5.64), 586 (4.49), 641 (4.52), 750 nm (4.27). HRMS–MALDI (*m/z*): [M + H]$^+$ calcd for $C_{72}H_{87}N_4S_4$, 1135.5814; found, 1135.5806. MS–MALDI *m/z* (% relative intensity, ion):

956 (100), 834 (84, M − 2SAr + H), 681 (78, M − 3SAr), 984 (56, M − SAr), 531 (23, M − 4SAr + H).

2,3,7,8,12,13,17,18-Octaethyl-5,10,15,20-tetrakis(naphthalen-2-ylthio)porphyrin 12: Porphyrin **1** (50 mg, 70 μmol, 1 equiv.), 2-naphthalenethiol (**HSAr**[8], 47 mg, 0.29 mmol, 4 equiv.) and TEA (3 drops) were reacted in chloroform (10 mL) at 25 °C for 5 min in which the color changed from brown to dark red. The solvent was removed *in vacuo* and column chromatography (SiO_2, hexane:ethyl acetate, 75:1–0:1, v/v) was performed. After elution of less polar side products, porphyrin **12** was obtained as a green solid upon removal of the solvent. Recrystallization by slow evaporation (hexane:ethyl acetate, 10:1, v/v) gave **12** as green crystals (40 mg, 46%). mp 168–170 °C dec. R_f 0.37 (SiO_2, hexane:ethyl acetate, 2:1, v/v). ^{1}H NMR (400.13 MHz, $CDCl_3$, δ) 0.93–1.15 (m, 12H), 1.39–1.64 (m, 12H), 2.50–3.57 (m, 16H), 6.83–7.14 (m, 8H), 7.28–7.41 (m, 8H), 7.41–7.49 (m, 4H), 7.50–7.63 (m, 8H). ^{13}C {^{1}H} NMR (100.61 MHz, $CDCl_3$, δ) 16.8, 20.1, 23.5, 24.8, 28.5, 36.7, 123.9, 124.7, 125.4, 126.6, 127.3, 127.9, 128.7, 131.6, 134.0, 140.0. UV (DCM) λ_{max} (log ε) 493 (5.32), 586 (4.18), 640 (4.20), 751 nm (4.05). HRMS–MALDI (*m/z*): $[M + H]^+$ calcd for $C_{76}H_{71}N_4S_4$, 1167.4562; found, 1167.4557. MS–MALDI *m/z* (% relative intensity, ion): 689 (100, M − 3SAr), 849 (84, M − 2SAr + H), 1008 (72, M – SAr + H), 531 (24, M − 4SAr + H).

2,3,7,8,12,13,17,18-Octaethyl-5,10,15,20-tetrakis[(pentafluorophenyl)thio]porphyrin 13: In a sample tube, H_2OETNP (**1**, 20 mg, 28 μmol, 1 equiv.) was dissolved in chloroform (3 mL). Then, perfluorobenzenethiol (**HSAr**[9], 25 mg, 0.12 mmol, 4.4 equiv.) and TEA (3 drops) were added and the solution was stirred at 25 °C for 5 min. To prevent consecutive decomposition of **13** with reactive species, the reaction mixture was washed with 3 × 10 mL of aqueous sodium hydroxide solution (2 M). The organic phase was dried using $MgSO_4$, filtered and the solvent was removed *in vacuo*. Column chromatography (SiO_2, hexane:ethyl acetate, 75:1–5:1, v/v) gave **13** as a green solid (15.9 mg, 43%) after separation of less polar side products. mp 86–87 °C dec. R_f 0.90 (SiO_2, hexane:ethyl acetate, 8:1, v/v). ^{1}H NMR (400.13 MHz, $CDCl_3$, δ) 1.07–1.18 (m, 24H), 2.97–3.42 (m, 16H). ^{13}C {^{1}H} NMR (100.61 MHz, $CDCl_3$,

δ) 16.1, 19.3, 34.9, 36.8, 46.4, 53.1, 108.2, 111.3, 111.5, 111.6, 117.8, 136.4, 138.9, 139.7, 142.2, 145.1, 147.6. ^{19}F NMR (376.59 MHz, $CDCl_3$, δ) −160.9 (s, 8F), −153.4 (s, 4F), −135.6 (s, 8F). UV (DCM) λ_{max} (log ε) 471 (4.68), 577 (3.69), 621 nm (3.76). HRMS–MALDI (*m/z*): $[M + H]^+$ calcd for $C_{60}H_{43}N_4S_4F_{20}$, 1327.2051; found, 1327.2039. MS–MALDI *m/z* (% relative intensity, ion): 150 (100), 729 (43, M − 3SAr), 929 (35, M − 2SAr + H), 531 (32, M − 4SAr + H), 1127 (31, M − SAr).

2,3,7,8,12,13,17,18-Octaethyl-5,10,15,20-tetrakis(phenanthren-9-ylthio)porphyrin 14: Porphyrin **1** (30 mg, 42 μmol, 1 equiv.) and 9-phenanthrenethiol (**HSAr[10]**, 39 mg, 0.19 mmol, 4.4 equiv.) were dissolved in chloroform (4 mL) and TEA (3 drops) was added. The mixture was then stirred at 25 °C until completion, as indicated by TLC analysis. After removal of the solvent at reduced pressure, the residue was chromatographed (SiO_2, hexane:ethyl acetate, 75:1–2:1, v/v) and the main fraction gave 10 mg (17%) of the green solid **14** after elution of less polar side products. mp 194–195 °C dec. R_f 0.40 (SiO_2, hexane:ethyl acetate, 3:1, v/v). ^{1}H NMR (400.13 MHz, $CDCl_3$, δ) 0.82–1.24 (m, 24H), 2.56–3.49 (m, 16H), 6.78–7.21 (m, 8H), 7.29–7.72 (m, 8H), 7.73–7.88 (m, 8H), 8.49–8.89 (m, 12H). ^{13}C {^{1}H} NMR (100.61 MHz, $CDCl_3$, δ) 16.8, 20.3, 24.8, 29.5, 31.1, 36.8, 53.9, 122.5, 123.4, 124.1, 126.1, 127.0, 127.3, 128.0, 128.8, 129.7, 130.7, 132.3, 138.8, 143.1. UV (DCM) λ_{max} (log ε) 490 (3.81), 495 (4.81), 642 nm (3.85). HRMS–MALDI (*m/z*): M^+ calcd for $C_{92}H_{78}N_4S_4$, 1366.5109; found, 1366.5090. MS–MALDI *m/z* (% relative intensity, ion): 950 (100), 1159 (92, M − SAr). 739 (73, M − 3SAr), 949 (41, M − SAr + H), 531.35 (17, M − 4SAr + H).

2,3,7,8,12,13,17,18-Octaethyl-5,10,15-tris[(4-methoxyphenyl)thio]porphyrin 15 and 2,3,7,8,12,13,17,18-octaethyl-5,10,15,20-tetrakis[(4-methoxyphenyl)thio]porphyrin 16: Porphyrin 1 (10 mg, 14 μmol, 1 equiv.), 4-methoxybenzenethiol (**HSAr[11]**, 8.4 mg, 60 μmol, 4 equiv.) and TEA (3 drops) were reacted in chloroform (2 mL) for 5 min at 25 °C During that time, the color changed from brown to red. Purification by preparative TLC (SiO_2, ethyl acetate) yielded an impure and inseparable mixture of the title compounds (combined yield <5%), as indicated by HRMS. **15**: HRMS–MALDI (*m/z*): $[M + H]^+$ calcd for $C_{57}H_{65}N_4O_3S_3$, 949.4213; found, 949.4241. **16**: HRMS–MALDI (*m/z*): M^+ calcd for

$C_{64}H_{71}N_4O_4S_4$, 1087.4358; found, 1087.4333.

{2,3,7,8,12,13,17,18-Octaethyl-5,10-dinitroporphyrinato}nickel(II) 18 and (2,3,7,8,12,13,17,18-octaethyl-10,15-dinitro-5-(pyridin-2-ylthio)porphyrinato}nickel(II) 19: Compound 1 (29 mg, 41 μmol, 1 equiv.), 2-mercaptopyridine (**HSAr[6]**, 18 mg, 0.16 mmol, 4 equiv.) and TEA (3 drops) were reacted in chloroform (5 mL) for 15 h at 25 °C after which another 4 equiv. of **HSAr[6]** were added. Completion of the reaction was then achieved after 15 minutes, as indicated by TLC analysis. The solvent was removed *in vacuo* and column chromatography (SiO_2, hexane:DCM, 2:1, v/v) was performed. After elution of less polar side products and unconsumed **1**, collection of the first major fraction gave the pink solid **18** (7.0 mg, 25%) upon removal of the solvent and recrystallization by slow evaporation (hexane:DCM, 10:1, v/v). A second column chromatography (SiO_2, hexane:ethyl acetate, 75:1, v/v) was performed with a mixture of the more polar fractions which yielded **19** (6.1 mg, 20%) after elution of impurities and removal of the solvent. **18**: mp > 300 °C. R_f 0.60 (SiO_2, hexane:DCM, 2:1, v/v). ^{1}H NMR (400.13 MHz, $CDCl_3$, δ) 1.36–1.47 (m, 12H), 1.67–1.77 (m, 12H), 3.40–3.51 (m, 8H), 3.73–3.84 (m, 8H), 9.53 (s, 2H). ^{13}C {^{1}H} NMR (100.61 MHz, $CDCl_3$, δ) 17.8, 17.9, 18.1, 18.2, 19.7, 20.2, 20.6, 98.5, 129.8, 131.7, 132.6, 141.7, 142.6, 142.8, 144.0, 145.3, 147.4. UV (DCM) λ_{max} (log ε) 400.13 (4.84), 531 (3.77), 567 nm (4.04). HRMS–MALDI (*m/z*): M^+ calcd for $C_{36}H_{42}N_6NiO_4$, 680.2621; found, 680.2627. **19**: mp 151–153 °C dec. R_f 0.13 (SiO_2, hexane:DCM, 2:1, v/v). ^{1}H NMR (400.13 MHz, $CDCl_3$, δ) 1.12–1.16 (m, 3H), 1.37–1.49 (m, 9H), 1.61–1.67 (m, 12H), 3.21–4.20 (m, 16H), 6.53–6.55 (m, 1H), 6.61–6.62 (m, 1H), 7.28 (s, 1H), 8.16–8.19 (m, 1H), 9.20 (s, 1H). ^{13}C {^{1}H} NMR (100.61 MHz, $CDCl_3$, δ) 17.2, 17.6 (x2), 17.7, 17.8, 17.9, 18.0, 19.4, 19.5, 20.0, 20.1, 20.2, 20.5, 22.1, 22.9, 98.6, 103.0, 119.3, 119.9, 129.7, 130.6 (x2), 131.4, 132.0, 132.6, 136.8, 140.7, 142.1, 143.2, 145.1, 145.7, 145.8, 146.1, 148.0, 148.6, 149.3, 149.6, 150.2, 163.1. UV (DCM) λ_{max} (log ε) 430 (4.40), 560 (3.43), 600 nm (3.57). HRMS–MALDI (*m/z*): M^+ calcd for $C_{41}H_{45}N_7NiO_4S$, 789.2607; found, 789.2629.

Denitration Reactions

2,3,7,8,12,13,17,18-Octaethyl-5,20-dinitroporphyrin 20[32] **and 2,3,7,8,12,13,17,18-octaethyl-5,15-dinitroporphyrin 21:**[32] 1,2-Ethanedithiol (**HSAr**[12], 19 mg, 0.2 mmol, 7 equiv.) and TEA (3 drops) were added to a solution of **1** (20 mg, 28 μmol, 1 equiv.) in chloroform (1.5 mL). After 40 min, the solvent was removed at reduced pressure and the crude product was purified *via* column chromatography (SiO_2, hexane:DCM, 2:1, v/v). The first fraction yielded **21** as a purple solid (3.7 mg, 21%). mp 282–284 °C (lit.[32] mp 280–282 °C) after removal of the solvent while the second fraction gave the purple solid **20** (4.2 mg, 24%). mp 227–230°C (lit.[32] mp 224–226 °C) upon evaporation of the solvent. A third fraction yielded tetrapyrrole **22** as a side product (<10%).

2,3,7,8,12,13,17,18-Octaethyl-5-nitroporphyrin 22:[32] Tetrapyrrole **1** (10 mg, 14 μmol, 1 equiv.) and 2-mercaptoethanol (**HSAr**[13], 13 mg, 0.17 mmol, 12 equiv.) were dissolved in DCM (2 mL) and TEA (3 drops) was added. After 15 min at 40 °C, the solvent was removed at reduced pressure and the crude product was purified by column chromatography (SiO_2, hexane:DCM, 2:1, v/v). This yielded the purple solid **22** (4.1 mg, 49%) upon removal of the solvent: mp 255–258 °C (lit.[32] mp 251–252 °C).

2,3,7,8,12,13,17,18-Octaethylporphyrin 23:[33] Porphyrin **1** (15 mg, 21 μmol, 1 equiv.) and benzyl mercaptan (**HSAr**[14], 107 mg, 0.86 mmol, 41 equiv.) were dissolved in 1.5 mL of DCM and TEA (0.1 mL) was added. This was allowed to react at 40 °C until completion, as indicated by TLC analysis (72 h). After removal of the solvent *in vacuo*, the crude product was purified *via* column chromatography (SiO_2, hexane:DCM, 2:1–1:1, v/v). A red band was collected to give tetrapyrrole **23** (5.5 mg, 49%): mp > 300 °C (lit.[33] mp 324–325 °C).

Crystallography

Crystal Structure Determinations. Crystals were grown following the protocol developed by Hope.[34] Diffraction data for all compounds were collected on a Bruker APEX 2 DUO CCD diffractometer by using graphite-monochromated MoK_α (λ = 0.71073

Å) radiation and Incoatec IμS CuK$_\alpha$ (λ = 1.54178 Å) radiation. Crystals were mounted on a MiTeGen MicroMount and collected at 100(2) K by using an Oxford Cryosystems Cobra low-temperature device. Data were collected by using omega and phi scans and were corrected for Lorentz and polarization effects by using the APEX software suite.[35] The structures were solved with Direct Methods and refined against $|F^2|$ with the program OLEX^2 by using all data.[36,37] Non-hydrogen atoms were refined with anisotopical thermal parameters. Hydrogen atoms were generally placed into geometrically calculated positions and refined using a riding model. The N-H hydrogen atoms were located using different maps and refined using the standard riding model. All images were rendered using XP in SHELXTL.[38]

Crystal data for 5,10,15,20-tetrakis[(4-bromophenyl)thio]-2,3,7,8,12,13,17,18-octaethylporphyrin 2: $C_{60}H_{58}Br_4N_4S_4$, M = 1282.98, tetragonal, $P\bar{4}2_1c$, a = 19.0974(9) Å, b = 19.0974(9) Å, c = 8.3204(4) Å, $\alpha = \beta = \gamma = 90°$, V = 3034.5(3) Å^3, T = 100.02 K, Z = 2, Z' = 0.25, μ(MoK$_\alpha$) = 2.830, 27514 reflections measured, 3487 unique (R_{int} = 0.0308) which were used in all calculations. The final wR_2 was 0.0630 (all data) and R_1 was 0.0278 (I > 2σ(I)). The structure was resolved as an inversion twin with one quarter molecule appearing in the asymmetric unit. The bromine unit was modelled over two parts using restraints (SADI, ISOR) in a 75–25% occupancy.

Crystal data for 2,3,7,8,12,13,17,18-octaethyl-5,10,15,20-tetrakis(phenylthio)porphyrin 9: $C_{60}H_{62}N_4S_4$, M = 967.37, monoclinic, $P2_1/n$, a = 8.9470(5) Å, b = 55.603(3) Å, c = 20.6784(10) Å, β = 91.7016(15)°, $\alpha = \gamma$ = 90 , V = 10282.6(9) Å^3, T = 100 K, Z = 8, Z' = 2, μ(MoK$_\alpha$) = 0.228, 101172 reflections measured, 21189 unique (R_{int} = 0.0506) which were used in all calculations. The final wR_2 was 0.1050 (all data) and R_1 was 0.0488 (I > 2σ(I)).

Crystal data for 2,3,7,8,12,13,17,18-octaethyl-5,10,15,20-tetrakis(pyridine-2-ylthio)porphyrin 10: $C_{56}H_{58}N_8S_4$, M = 971.34, orthorhombic, $P2_12_12_1$, a = 8.7585(5) Å, b = 23.2617(14) Å, c = 24.6838(14) Å, $\alpha = \beta = \gamma = 90°$, V = 5029.0(5) Å^3, T = 100(2) K, Z = 4, Z' = 1, μ(CuK$_\alpha$) = 2.095, 60358 reflections measured, 9224 unique (R_{int} = 0.1181)

which were used in all calculations. The final wR_2 was 0.1773 (all data) and R_1 was 0.0656 (I > 2σ(I)).

Crystal data for 2,3,7,8,12,13,17,18-octaethyl-5,20-dinitroporphyrin 20: $C_{36}H_{44}N_6O_4$, M = 624.77, monoclinic, $P2_1/c$, a = 12.7085(6) Å, b = 10.9353(5) Å, c = 23.2462(11) Å, β = 92.6748(15)°, α = γ = 90°, V = 3227.0(3) Å^3, T = 100 K, Z = 4, Z' = 1, μ(MoK$_\alpha$) = 0.085, 33510 reflections measured, 6660 unique (R_{int} = 0.0641) which were used in all calculations. The final wR_2 was 0.1158 (all data) and R_1 was 0.0471 (I > 2σ(I)).

Crystal data for 2,3,7,8,12,13,17,18-octaethyl-5,15-dinitroporphyrin 21: $C_{36}H_{44}N_6O_4$, M = 624.77, triclinic, $P\bar{1}$, a = 9.6015(5) Å, b = 13.6688(8) Å, c = 13.7637(8) Å, α = 101.568(3)°, β = 106.044(2)°, γ = 104.705(2)°, V = 1606.37(16) Å^3, T = 100 K, Z = 2, Z' = 1, μ(MoK$_\alpha$) = 0.086, 26989 reflections measured, 6283 unique (R_{int} = 0.0814) which were used in all calculations. The final wR_2 was 0.1167 (all data) and R_1 was 0.0480 (I > 2σ(I)).

Crystal data for 2,3,7,8,12,13,17,18-octaethyl-5,10,15-trinitroporphyrin 32: $C_{36}H_{43}N_7O_6$, M = 669.77, orthorhombic, $P2_12_12_1$, a = 8.6656(11) Å, b = 13.9561(17) Å, c = 27.365(3) Å, α = β = γ = 90°, V = 3309.5(7) Å^3, T = 100 K, Z = 4, Z' = 1, μ(MoK$_\alpha$) = 0.093, 45306 reflections measured, 7236 unique (R_{int} = 0.0572) which were used in all calculations. The final wR_2 was 0.1000 (all data) and R_1 was 0.0411 (I > 2σ(I)).

Crystal data for {2,3,7,8,12,13,17,18-octaethyl-5,10-dinitroporphyrinato}nickel(II) 18: $C_{36}H_{42}N_6NiO_4$, M = 681.46, monoclinic, $P2_1/c$, a = 9.5646(4) Å, b = 23.0982(9) Å, c = 14.9997(6) Å, β = 93.453(2)°, α = γ = 90°, V = 3307.8(2) Å^3, T = 100 K, Z = 4, Z' = 1, μ(CuK$_\alpha$) = 1.243, 61642 reflections measured, 6026 unique (R_{int} = 0.0883) which were used in all calculations. The final wR_2 was 0.1240 (all data) and R_1 was 0.0451 (I > 2σ(I)). The nitro group in at the C5 position was modelled over two positions with 58–42% occupancy.

Normal structural decomposition (NSD) analysis. The theoretical background and development of this method have been described by Shelnutt *et al*.[20] NSD is a conceptually simple method that employs the decomposition of the conformation of the macrocycle by a basis set composed of its various normal modes of vibration, affording clear separation of the contributing distortions to the macrocycle conformation in a quantitative fashion. For calculations, we used the NSD engine program established by Shelnutt.[39]

ASSOCIATED CONTENT

Supporting Information: A quantitative study on the influence of TEA on the consumption of **1**, NMR spectra of the reaction products, crystal data for **12**, and the UV-Vis spectra of **1**, **20**, **21**, **22**, **23**, and **32**. This material is available free of charge via the Internet at http://pubs.acs.org. CCDC 1499410, 1499411, 1532226–1532231 contain the supplementary crystallographic data for this paper. These data can be obtained free of charge from The Cambridge Crystallographic Data Centre *via* www.ccdc.cam.ac.uk/data_request/cif.

AUTHOR INFORMATION

Corresponding Author
* E-mail: sengem@tcd.ie.

ACKNOWLEDGMENT

This work was supported by a grant from Science Foundation Ireland (SFI IvP 13/IA/1894).

REFERENCES

(1) Senge, M. O. *Acc. Chem. Res.* **2005**, *38*, 733.
(2) Gong, L.-C.; Dolphin, D. *Can. J. Chem.* **1985**, *63*, 406.

(3) (*a*) Zhu, N.-J.; Li, Y.; Wu, G.-Z.; Liang, X.-G. *Acta Chim. Sin.* **1992**, *50*, 249; (*b*) Senge, M. O.; Eigenbrot, C. W.; Brennan, T. D.; Shusta, J.; Scheidt, W. R.; Smith, K. M. *Inorg. Chem.* **1993**, *32*, 3134; (*c*) Senge, M. O. *J. Chem. Soc., Dalton Trans.* **1993**, 3539; (*d*) Senge, M. O.; Smith, K. M. *J. Chem. Soc., Chem. Commun.* **1994**, 923; (e) Patra, R.; Bhowmik, S.; Ghosh, S. K.; Rath, S. P. *Dalton Trans.* **2010**, *39*, 5795; (f) Pukhoskaya, S.; Ivanova, Y.; Nam, D. T.; Vashurin, A.; Golubchikov, O. *J. Porphyrins Phthalocyanines* **2015**, *19*, 858.

(4) Devillers, C. H.; Hebié, S.; Lucas, D.; Cattey, H.; Clément, S.; Richeter, S. *J. Org. Chem.* **2014**, *79*, 6424.

(5) (*a*) Cogolli, P.; Maiolo, F.; Testaferri, L.; Tingolo, M.; Tiecco, M. *J. Org. Chem.* **1979**, *44*, 2642; (*b*) Montanari, S.; Paradisi, C.; Scorrano, G. *J. Org. Chem.* **1993**, *58*, 5628; (*c*) Hartwig, J. F. *Nature* **2008**, *455*, 314; (*d*) Sreedhar, B.; Reddy, P S.; Reddy, M. A. *Synthesis* **2009**, 1732; (*e*) Hoyle, C. E.; Bowman, C. N. *Angew. Chem.* **2010**, *122*, 1584; *Angew. Chem. Int. Ed.* **2010**, *49*, 1540; (*f*) Xu, H.-J.; Zhao, Y.-Q.; Feng, T.; Feng, Y.-S. *J. Org. Chem.* **2012**, *77*, 2878.

(6) (*a*) Yamashita, K.-I.; Kataoka, K.; Asano, M. S.; Sugiura, K.-i. *Org. Lett.* **2012**, *14*, 190; (*b*) Ryan, A. A.; Plunkett, S.; Casey, A.; McCabe, T.; Senge, M. O. *Chem. Commun.* **2014**, *50*, 353; (*c*) Chen, Q.; Zhu, Y.-Z.; Fan, Q. J.; Zhang, S.-C.; Zheng, J.-Y. *Org. Lett.* **2014**, *16*, 1590.

(7) (*a*) Baldwin, J. E.; Crossley, M. J.; DeBernardis, J. *Tetrahedron* **1982**, *38*, 685; (*b*) Crossley, M. J.; Lionel, G.; Pyke, S. M.; Charles, W. *J. Porphyrins Phthalocyanines* **2002**, *16*, 685.

(8) (*a*) Senge, M. O. *Chem. Commun.* **2006**, 243; (*b*) Senge, M. O.; MacGowan, S. A.; O'Brien, J. M. *Chem. Commun.* **2015**, *51*, 17031.

(9) Radi, R.; Beckman, J. S.; Bush, K. M.; Freeman, B. A. *J. Biol. Chem.* **1991**, *266*, 4244.

(10) (*a*) Hutchison, J. E.; Postlethwaite, T. A.; Murray, R. W. *Langmuir* **1993**, *9*, 3277; (*b*) Shimazu, K.; Takechi, M.; Fujii, H.; Suzuki, M.; Saiki, H.; Yoshimura, T.; Uosaki, K. *Thin Solid Films* **1996**, *273*, 250; (*c*) Clausen, C.; Gryko, D. T.; Dabke, R. B.; Dontha, N.; Bocian, D. F.; Kuhr, W. G.; Lindsey, J. S. *J. Org. Chem.* **2000**, *65*, 7363; (*d*) Clausen, C.;

Gryko, D. T.; Yasseri, A. A.; Diers, J. R.; Bocian, D. F.; Kuhr, W. G.; Lindsey, J. S. *J. Org. Chem.* **2000**, *65*, 7371.

(11) Copley, G.; Shimizu, D.; Oh, J.; Sung, J.; Furukawa, K.; Kim, D.; Osuka, A. *Eur. J. Org. Chem.* **2016**, 1977.

(12) Crossley, M. J.; Gosper, J. J.; Wilson, M. G. *J. Chem. Soc., Chem. Commun.* **1985**, 1798.

(13) (*a*) Jackson, C. J.; Gazzolo, F. H. *J. Chem. Soc.* **1900**, *23*, 376; (*b*) Meisenheimer, J. *Justus Liebigs Ann. Chem.* **1902**, *323*, 205.

(14) (*a*) Stolzenberg, A. M.; Stershic, M. T. *J. Am. Chem. Soc.* **1988**, *110*, 6391; (*b*) Bhyrappa, P.; Krishnan, V. *Inorg. Chem.* **1991**, *30*, 239.

(15) Yamamoto, Y.; Yamamoto, A.; Furuta, S.-y.; Horie, M.; Kodama, M.; Sato, W.; Akiba, K.-y.; Tsuzuki, S.; Uchimaru, T.; Hashizume, D.; Iwasaki, F. *J. Am. Chem. Soc.* **2005**, *127*, 14540.

(16) Medforth, C. J.; Senge, M. O.; Smith, K. M.; Sparks, L. D.; Shelnutt, J. A., *J. Am. Chem. Soc.* **1992**, *114*, 9859.

(17) Kadish, K. M.; Lin, M.; Caemelbecke, E. V.; De Stefano, G.; Medforth, C. J.; Nurco, D. J.; Nelson, N. Y.; Krattinger, B.; Muzzi, C. M.; Jaquinod, L.; Xu, Y.; Shyr, D. C.; Smith, K. M.; Shelnutt, J. A. *Inorg. Chem.* **2002**, *41*, 6673.

(18) Lauher, J. W.; Ibers, J. A. *J. Am. Chem. Soc.* **1973**, *95*, 5148.

(19) Silvers, S. J.; Tulinsky, A. *J. Am. Chem. Soc.* **1967**, *89*, 3331.

(20) (*a*) Jentzen, W.; Simpson, M. C.; Hobbs, J. D.; Song, X.; Ema, T.; Nelson, N. Y.; Medforth, C. J.; Smith, K. M.; Veyrat, M. *J. Am. Chem. Soc.* **1995**, *117*, 11085; (*b*) Jentzen, W.; Song, X.; Shelnutt, J. A. *J. Phys. Chem. B* **1997**, *101*, 1684; (*c*) Jentzen, W.; Ma, J.; Shelnutt, J. A. *Biophys. J.* **1998**, *74*, 753.

(21) Clezy, P. S.; Craig, D. C.; James, V. J.; McConnell, J. F.; Rae, A. D. *Cryst. Struct. Commun.* **1979**, *8*, 605.

(22) Barkigia, K. M.; Palacio, M.; Sun, Y.; Nogues, M.; Renner, M. W.; Varret, F.; Battioni, P.; Mansuy, D.; Fajer, J. *Inorg. Chem.* **2002**, *41*, 5647.

(23) Schaefer, W. P.; Ellis, P. E.; Lyons, J. E.; Shaikh, S. N. *Acta Cryst.* **1995**, C*51*, 2252.

(24) Patra, R.; Chaudhary, A.; Ghosh, S. K.; Rath, S. P. *Inorg. Chem.* **2008**, *47*, 8324.

(25) Haddad, R.; Lu, Y.; Quirke, J. M. E.; Berget, P.; Sun, L.; Fettinger, J. C.; Leung, K.; Qiu, Y.; Schore, N. E.; van Swol, F.; Medforth, C. J.; Shelnutt, J. A. *J. Porphyrins Phthalocyanines* **2011**, *15*, 727.

(26) Senge, M. O.; Bischoff, I. *Eur. J. Org. Chem.*, **2001**, 1735.

(27) Medforth, C. J.; Senge, M. O.; Forsyth, T. P.; Hobbs, J. D.; Shelnutt, J. A.; Smith, K. M. *Inorg*. *Chem*. **1994**, *33*, 3865.

(28) Watanabe, E.; Nishimura, S.; Ogoshi, H.; Yoshida, Z. *Tetrahedron* **1975**, *31*, 1385.

(29) Giarrusso, M. A.; Taylor, M. K.; Ziogas, J.; Brody, K. M.; MacDougall, P. E.; Schiesser, C. H. *Asian J*. *Org*. *Chem*. **2012**, *1*, 274.

(30) Šindelář, K.; Holubek, J.; Ryska, M.; Koruna, I.; Protiva, M. *Collect*. *Czech*. *Chem*. *Comm*. **1986**, *51*, 2848.

(31) (*a*) Ali, H.; van Lier, J. E. *Tetrahedron Lett*. **1991**, *32*, 5015; (*b*) Hobbs, J. D.; Majumder, S. A.; Luo, L.; Sickelsmith, G. A.; Quirke, J. M. E.; Medforth, C. J.; Smith, K. M.; Shelnutt, J. A. *J. Am*. *Chem. Soc*. **1994**, *116*, 3261.

(32) Bonnett, R.; Stephenson, G. F. *J. Org*. *Chem*. **1965**, *30*, 2791.

(33) Whitlock Jr., H. W.; Hanauer, R. *J. Org. Chem.* **1968**, *33*, 2169.

(34) Hope, H. *Prog*. *Inorg*. *Chem*. **1994**, *41*, 1.

(35) Bruker. (2014). SAINT, APEX2 and SADABS. Bruker AXS Inc., Madison, Wisconsin, USA.

(36) Dolomanov, O. V.; Bourhis, L. J.; Gildea, R. J.; Howard J. A. K.; Puschmann, H. *J*. *Appl*. *Cryst*., **2009**, *42*, 339.

(37) Sheldrick, G. M. *Acta Cryst*., **2015**, A*71*, 3.

(38) Sheldrick, G. M. *Acta Cryst*., **2008**, A*64*, 112.

(39) NSDGUI. (2001), Version 1.3 alpha version, Sandia National Laboratory, New Mexico, USA.

Table of Contents (TOC):